Insights into dimethyl sulfoxide decomposition in Li-O$_2$ battery: Understanding carbon dioxide evolution

Nataliia Mozhzhukhina, Florencia Marchini, Walter R. Torres, Alvaro Y. Tesio, Lucila P. Mendez De Leo, Federico J. Williams, Ernesto J. Calvo*

Departamento de Química Inorgánica, Analítica y Química Física, INQUIMAE-CONICET, Facultad Ciencias Exactas y Naturales, Universidad de Buenos Aires, Ciudad Universitaria, Pabellón 2, Buenos Aires C1428EHA, Argentina

ARTICLE INFO

ABSTRACT

DMSO has been widely investigated as a potential electrolyte for the Li-air battery systems, however its stability has been a topic of debate in the research community. In this communication we have identified the side reaction products during the oxygen reduction reaction (ORR) and oxygen evolution reaction (OER) on Au in dimethyl sulfoxide-based electrolyte for Li-air battery by a combination of in-situ analytical tools: EQCM, SNIFTIRS, DEMS and XPS, in particular the evolution of CO$_2$ from the solvent decomposition.

1. Introduction

Li-air battery has attracted much research attention recently; however the electrolyte instability still remains one of the biggest challenges [1,2,3,4,5]. Dimethyl sulfoxide (DMSO) has been suggested as a possible stable electrolyte due to the increased stability of the superoxide anion in this solvent [6]; Li-air battery testing utilizing DMSO as a solvent has also shown an improved performance [7,8]. But, there has been some controversy on its stability. Schroeder et al. [9] have reported that DMSO is stable under operating conditions in Li-air batteries. However, several studies later have questioned DMSO stability [10,11,12], reporting side products such as LiOH [13,14], dimethyl sulfone [13,14,15], Li$_2$SO$_3$ [13] and Li$_2$SO$_4$ [14]. While DMSO might not be a stable solvent, it does possess unique properties, such as stabilization of superoxide anion [6,16,17] and therefore is very interesting solvent from a fundamental point of view.

In this communication we report a new insight on the decomposition of DMSO-based solvent for Li-O$_2$ system evidenced by in-situ analytical tools (SNIFTIRS, EQCM, DEMS and XPS) coupled to the electrochemical cell. We have also used the TBA$^+$ cation along with Li$^+$ in order to distinguish separately the effects on solvent decomposition from different reactive species and reaction components: O$_2$, O$_2^-$, Li$^+$, Li$_2$O$_2$, etc.

2. Experimental

Anhydrous dimethyl sulfoxide, $\geq 99.9\%$ (276855 SIGMA-Aldrich), tetrabutylammonium hexafluorophosphate for electrochemical analysis, $\geq 99.0\%$ (86879 Fluka), lithium hexafluorophosphate battery grade, $\geq 99.99\%$ trace metals basis (450227 Aldrich), were stored in the argon-filled MBRAUN glove box with an oxygen content ≤ 0.1 ppm and water content below 2 ppm. All solutions were prepared inside the glove box and the water content was measured using the Karl Fisher 831 KF Coulometer (Metrohm). Solutions were found to contain around 20 ppm of water.

Electrochemical in situ subtractively normalized interfacial Fourier transform infrared spectroscopy (SNIFTIRS) experiments were carried out on a Thermo Nicolet 8700 (Nicolet, Madison, WI) spectrometer equipped with a custom-made external tabletop optical mount, an MCTA detector, and a custom-made Teflon electro-chemical cell. The cell design has been described in detail elsewhere [18]..

Differential electrochemical mass spectrometry (DEMS) was accomplished using a Pfeiffer vacuum Omnistar GSD 320 gas analysis system with a quadrupole mass spectrometer QGM 220 (mass range 1–200 amu) with ion gastight ion source, yttriated iridium-filament with secondary electron multiplier C-SEM and Faraday detectors. The DEMS cell setup was used as described elsewhere [18].

Electrochemical quartz crystal microbalance measurements was carried out acquiring a crystal admittance spectra in the vicinity of the fundamental resonant frequency by using a Hewlett Packard HP

---

* Corresponding author.
  E-mail address: calvo@qi.fcen.uba.ar (E.J. Calvo).

E5100A network analyzer connected to the quartz crystal in the Teflon electrochemical cell through 50 Ω coaxial matched cables (HP10502A) via a HP 41900A π-Network test fixture with rigid brass connectors to the crystal. The HP E5100A network analyzer was interfaced to a computer via Agilent 82357B USB/GPIB interface and the electrochemical cell was controlled with a grounded working electrode by means of an operational amplifier potentiostat/galvanostat with special software developed in our laboratory using Labview 10.0, the electrochemical current was measured at the auxiliary electrode and both current and potential signals were acquired by 2 Agilent 34410 61/2 digit multimeters by USB interfaces. The network analyzer was calibrated prior to each measurement by 3-term calibration: open, close and 50 Ω. The acoustic admittance spectra of the Au covered quartz crystal were recorded at 1.5 s intervals simultaneous to current and potential signals.

XPS measurements were performed using an SPECS GmbH ultrahigh vacuum (UHV) chamber which counts with a transfer system for rapid and controlled transfer of the sample between the UHV environment and the liquid non aqueous electrolyte containing either Ar or O_2 gas at atmospheric pressure. The EC-UHV transfer system has been described elsewhere [19]. High purity polycrystalline gold sample was Ar^+ sputtered and annealed in subsequent cycles until no impurities were detected by XPS.

3. Results and discussion

For the in situ SNIFTIRS experiment, a set of fixed potentials was chosen according to CV in DMSO and was applied to the cathode. The IR spectra were collected at each potential applied in order to evaluate changes produced on the electrode surface. Potentials were chosen in order to follow the cyclic voltammetry and to observe ORR first and then OER. We have performed the in situ IR measurements in the Li^+ containing and O_2 saturated DMSO, in TBA^+ containing and O_2 saturated DMSO and also in TBA^+ containing O_2 free solution. Those measurements allowed us to separate the different reactive species, Li^+ and O_2, and to elucidate their effect on the decomposition reaction. Previously we have reported dimethyl sulfone formation in similar experiments [15].

The resulting spectra for the solutions of $LiPF_6$ and $TBAPF_6$ in oxygenated DMSO are shown in the Fig. 1. Notably from a potential of 4.2 V and above, a downward peak is detected at 2340 cm^{-1} and corresponds to antisymmetric stretching of CO_2 in the vicinity of the electrode surface. The CO_2 evolution has been detected in the oxygenated solutions of DMSO at high potentials, either with or without Li^+. However, practically no CO_2 evolution from the deoxygenated DMSO has been detected (data not shown). This is an evidence of an important role of molecular oxygen for the solvent decomposition consistent with
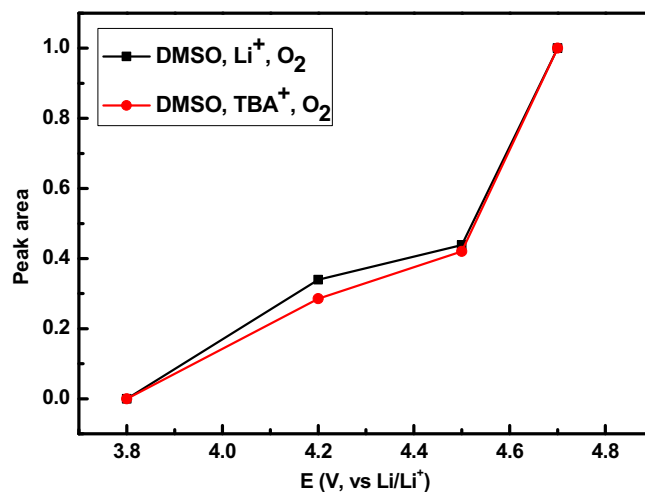

Fig. 2. CO_2 peak integrated area versus applied potential in solution of 0.1 M $LiPF_6$ in DMSO 0.1 M $TBAPF_6$ in DMSO, saturated in O_2 on a Au working electrode.

the DEMS results demonstrating oxygen depletion during CO_2 evolution and gold porous electrode [10].

The normalized integrated peak area of carbon dioxide peak at 2340 cm^{-1} versus applied potential is shown in Fig. 2 for the oxygenated DMSO solutions with and without Li^+. It can be seen that in both solutions CO_2 evolution starts at around 4.2 V and it is notable that the CO_2 evolution pattern is almost identical in the solution containing Li^+ and TBA^+.

In the potentiostatic experiments coupled to the quartz crystal microbalance and mass spectroscopy, three different potentials: 1.9 V, 3.1 and 4.5 V, were applied for 2 min to the gold working electrode and the responses of EQCM and DEMS were measured accordingly. The results are depicted simultaneously on the Fig. 3. When 1.90 V was applied to the cell, the EQCM showed a mass increase up to 5.5 μg, and at the same time DEMS signal for ionic current m/q = 32 (O_2) decreased. When the potential of cell was switched to 3.1 V, the mass in EQCM remained unaffected, but O_2 signal showed a peak, that decreased gradually with time. Finally, when the cell potential was set to 4.5 V, the mass measured by EQCM decayed completely until reaching the initial experimental value. At the same time the signal of CO_2 in DEMS increased considerably, while the O_2 signal remained constant. To conclude, during the potential of 1.9 V, we evidenced a mass increase simultaneous to the oxygen consumption that corresponds the ORR. At 3.1 V the oxygen was evolved, while the mass remained the same, thus we suggest that only soluble species (superoxide anion) are oxidized at this potential. At 4.5 V we saw disappear-
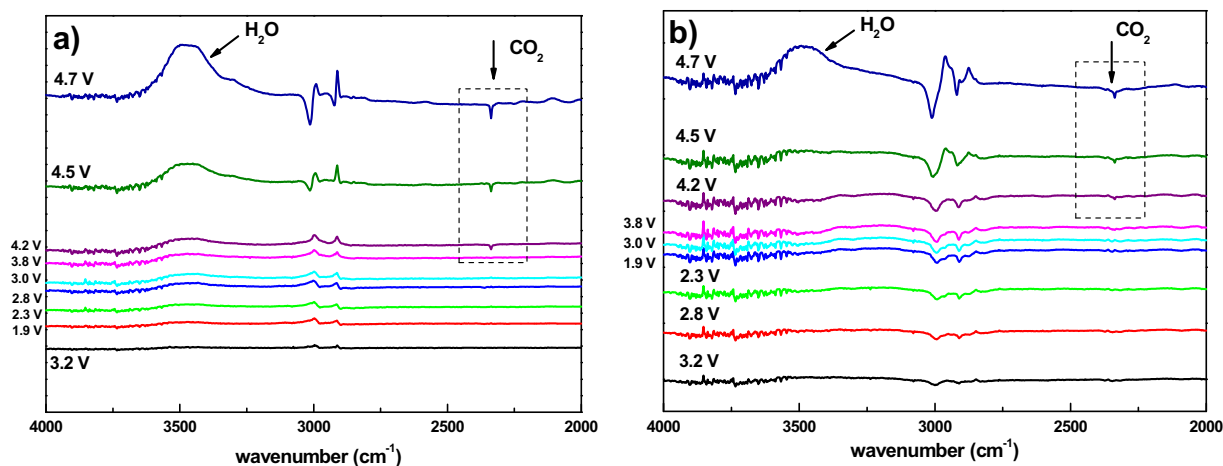

Fig. 1. In situ IR spectra of solutions a) 0.1 M $LiPF_6$, DMSO, O_2 saturated and b) 0.1 M $TBAPF_6$, DMSO, O_2 saturated.
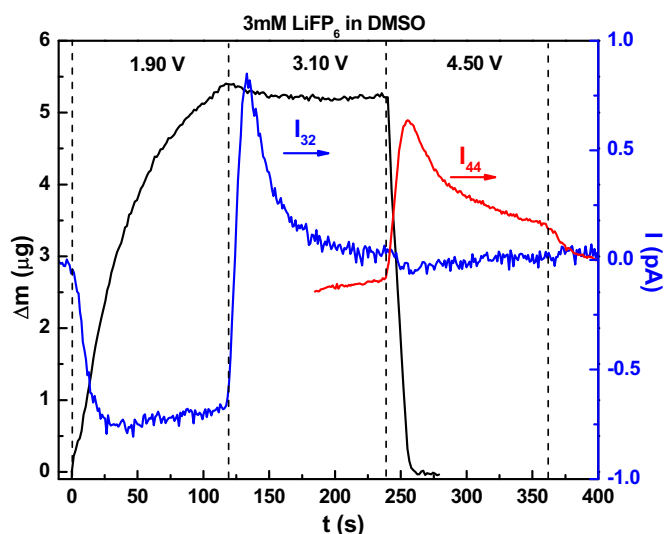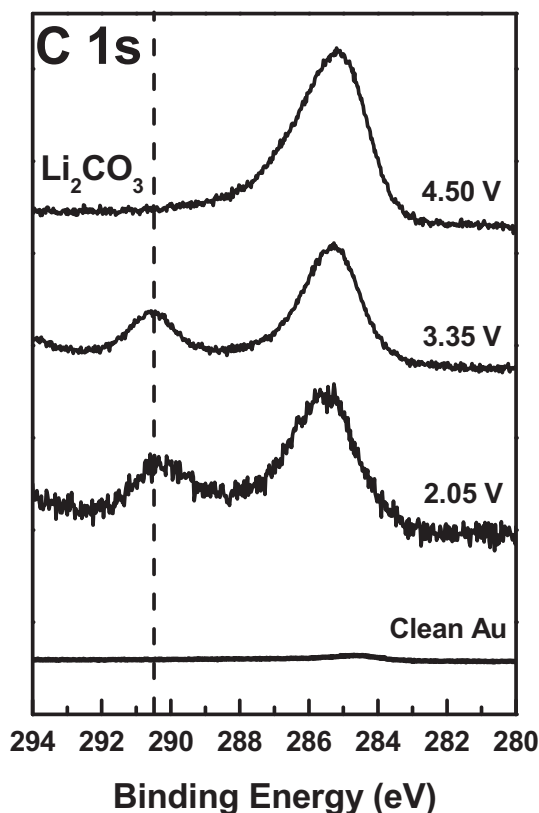
Fig. 3. DEMS and EQCM.

Fig. 4. C1s region of XPS spectra performed on a clean gold electrode and after polarization at 2.05 V, 3.35 V and 4.40 V in a DMSO/LiPF$_6$ O$_2$ saturated electrolyte.

ance of mass in EQCM, however only CO$_2$ was evolved at this potential and no O$_2$ evolution occurred, suggesting that other then lithium peroxide species are oxidized at this potential.

To identify the nature of the deposit detected by EQCM, we have also performed XPS measurements on a clean gold electrode and after polarization at the selected potentials of 2.05 V, 3.35 V and 4.50 V, which correspond to ORR potential, the thermodynamic redox potential of Li/Li$_2$O$_2$ couple and OER potential respectively. The XPS signals of the C 1s region are presented in the Fig. 4. Whereas no carbon was initially present on the surface of the electrode, two broad peaks centered at 285.4 eV and 290.5 eV appeared after performing the ORR at 2.05 V. The peak at 285.4 eV is a complex signal which can be

attributed to a number of R-O species, while the signal at 290.5 eV is typical from carbonate anion.

As for the attempts to restore the surface through anodic polarizations, electrochemical oxidation at 4.50 eV only succeeded to remove lithium carbonate, whereas the other carbon species remained on the surface. Those results are in agreement with SNIFTIRS and DEMS results that detect CO$_2$ formation at the same potential.

As the only carbon containing compound of the system was the solvent, these results support the idea that DMSO undergoes further chemical decomposition after reacting with ORR products and no full recharge is possible owing to the remaining species on the surface of the electrode even after highly oxidizing polarization. The observed spectroscopic S2p, Li1s and O1s regions strongly complements this hypothesis [10]. The finding is in agreement with work published by Younesi et al. [12], who reported the decomposition of DMSO in direct contact with Li$_2$O$_2$ powder by XPS.

While the exact mechanism for the degradation of the solvent DMSO has not been completely unraveled, at this point in time we have clear evidence of carbonate and other oxygenated carbonaceous mater formation on the surface during ORR and direct electro-chemical oxidation to dimethyl sulphone [15] at high overpotential. Furthermore both IR and DEMS have revealed two sources of CO$_2$, from carbonate decomposition and from solvent oxidation at high overvoltage. Also XPS has shown formation of sulfur species on the surface [10].

4. Conclusions

We have combined several analytical in situ tools in order to get a deeper insight into the decomposition of DMSO in conditions relevant to the Li-air battery operation. During the ORR we have shown new evidence of mass increase by EQCM simultaneous to the oxygen consumption by DEMS. However, by XPS we have shown that this deposit was not only the desired Li$_2$O$_2$ but also carbonates and a number of R-O species were formed. At a potential of 3.1 V we detected the oxygen evolution in solution of 3 mmol of Li$^+$ in DMSO, however the mass remained the same and the XPS has shown that carbonates and R-O species remained on the surface. However when applying a high potential of 4.5 V the mass decreased simultaneously to the disappearance of carbonates and the CO$_2$ evolved as evidenced both by DEMS and SNIFTIRS. However interestingly enough, infrared spectroscopy studies have shown the formation of CO$_2$ also in the absence of Li$^+$ ion, while the presence of oxygen was necessary to result in CO$_2$ evolution. All this evidence suggests that lithium peroxide undergoes decomposition reaction with DMSO forming lithium carbonate that can only be oxidized at high potential of 4.5 V resulting in evolution of carbon dioxide; other parasitic reaction of solvent with molecular oxygen also can occur resulting in CO$_2$ evolution.

Acknowledgements

References

[1] D. Aurbach, B.D. McCloskey, L.F. Nazar, P.G. Bruce, Advances in understanding mechanisms underpinning lithium–air batteries, Nat. Energy 1 (2016) 16128.
[2] K. Amine, R. Kanno, Y. Tzeng, Rechargeable lithium batteries and beyond: progress, challenges, and future directions, MRS Bull. 39 (05) (2014) 395–401.
[3] L. Grande, E. Paillard, J. Hassoun, J.B. Park, Y.J. Lee, Y.K. Sun, S. Passerini, B. Scrosati, The lithium/air battery: still an emerging system or a practical reality? Adv. Mater. 27 (5) (2015) 784–800.
[4] A.C. Luntz, B.D. McCloskey, Nonaqueous Li-air batteries: a status report, Chem. Rev. 114 (23) (2014) 11721–11750.
[5] B.D. McCloskey, C.M. Burke, J.E. Nichols, S.E. Renfrew, Mechanistic insights for the development of Li-O$_2$ battery materials: addressing Li$_2$O$_2$ conductivity limitations

and electrolyte and cathode instabilities, Chem. Commun. 51 (64) (2015) 12701–12715.

[6] M.J. Trahan, S. Mukerjee, E.J. Plichta, M.A. Hendrickson, K.M. Abraham, Studies of Li-air cells utilizing dimethyl sulfoxide-based electrolyte, J. Electrochem. Soc. 160 (2) (2012) A259–A267.

[7] Z. Peng, S.A. Freunberger, Y. Chen, P.G. Bruce, A reversible and higher-rate Li-O$_2$ battery, Science 337 (6094) (2012) 563–566.

[8] W. Xu, J. Hu, M.H. Engelhard, S.A. Towne, J.S. Hardy, J. Xiao, J. Feng, M.Y. Hu, J. Zhang, F. Ding, M.E. Gross, J.-G. Zhang, The stability of organic solvents and carbon electrode in nonaqueous Li-O$_2$ batteries, J. Power Sources 215 (2012) 240–247.

[9] M.A. Schroeder, N. Kumar, A.J. Pearse, C. Liu, S.B. Lee, G.W. Rubloff, K. Leung, M. Noked, DMSO-Li$_2$O$_2$ interface in the rechargeable Li-O$_2$ battery cathode: theoretical and experimental perspectives on stability, ACS Appl. Mater. Interfaces 7 (21) (2015) 11402–11411.

[10] F. Marchini, S. Herrera, W. Torres, A.Y. Tesio, F.J. Williams, E.J. Calvo, Surface study of lithium-air battery oxygen cathodes in different solvent-electrolyte pairs, Langmuir 31 (33) (2015) 9236–9245.

[11] F. Marchini, S.E. Herrera, E.J. Calvo, F.J. Williams, Surface studies of lithium–oxygen redox reactions over HOPG, Surf. Sci. 646 (2016) 154–159.

[12] R. Younesi, P. Norby, T. Vegge, A new look at the stability of dimethyl sulfoxide and acetonitrile in Li-O$_2$ batteries, ECS Electrochem. Lett. 3 (3) (2014) A15–A18.

[13] D.G. Kwabi, T.P. Batcho, C.V. Amanchukwu, N. Ortiz-Vitoriano, P. Hammond, C.V. Thompson, Y. Shao-Horn, Chemical instability of dimethyl sulfoxide in lithium-air batteries, J. Phys. Chem. Lett. 5 (16) (2014) 2850–2856.

[14] D. Sharon, M. Afri, M. Noked, A. Garsuch, A.A. Frimer, D. Aurbach, Oxidation of dimethyl sulfoxide solutions by electrochemical reduction of oxygen, J. Phys. Chem. Lett. 4 (18) (2013) 3115–3119.

[15] N. Mozhzhukhina, L.P. Méndez De Leo, E.J. Calvo, Infrared spectroscopy studies on stability of dimethyl sulfoxide for application in a Li–air battery, J. Phys. Chem. C 117 (36) (2013) 18375–18380.

[16] E.J. Calvo, N. Mozhzhukhina, A rotating ring disk electrode study of the oxygen reduction reaction in lithium containing non aqueous electrolyte, Electrochem. Commun. 31 (2013) 56–58.

[17] W. Torres, N. Mozhzhukhina, A.Y. Tesio, E.J. Calvo, A rotating ring disk electrode study of the oxygen reduction reaction in lithium containing dimethyl sulfoxide electrolyte: role of superoxide, J. Electrochem. Soc. 161 (14) (2014) A2204–A2209.

[18] N. Mozhzhukhina, A.Y. Tesio, L.P.M. De Leo, E.J. Calvo, In situ infrared spectroscopy study of PYR14TFSI ionic liquid stability for Li–O$_2$ battery, J. Electrochem. Soc. 164 (2) (2017) A518–A523.

[19] L.P.M. De Leo, E. De La Llave, D. Scherlis, F.J. Williams, Molecular and electronic structure of electroactive self-assembled monolayers, J. Chem. Phys. 138 (11) (2013).